http://www.jstage.jst.go.jp/browse/biophysics

BIOPHYSICS

REVIEW

Vol. 10, pp. 69–75 (2014)
doi: 10.2142/biophysics.10.69

Myosin V is a biological Brownian machine

Keisuke Fujita[1] and Mitsuhiro Iwaki[1,2]

[1]*Quantitative Biology Center, RIKEN, Suita, Osaka 565-0874, Japan*
[2]*Graduate School of Frontier Biosciences, Osaka University, Suita, Osaka 565-0871, Japan*

Received September 1, 2014; accepted October 8, 2014

Myosin V is a vesicle transporter that unidirectionally walks along cytoskeletal actin filaments by converting the chemical energy of ATP into mechanical work. Recently, it was found that myosin V force generation is a composition of two processes: a lever-arm swing, which involves a conformational change in the myosin molecule, and a Brownian search-and-catch, which involves a diffusive "search" by the motor domain that is followed by an asymmetric "catch" in the forward actin target such that Brownian motion is rectified. Here we developed a system that combines optical tweezers with DNA nanomaterial to show that the Brownian search-and-catch mechanism is the energetically dominant process at near stall force, providing 13 k_BT of work compared to just 3 k_BT by the lever-arm swing. Our result significantly reconsiders the lever-arm swinging model, which assumes the swing dominantly produces work (>10 k_BT), and sheds light on the Brownian search-and-catch as a driving process.

Key words: Brownian motor, myosin, motor protein, nano machine

Myosin V is a dimeric motor protein that transports various cargos such as melanosomes, endoplasmic reticulum and messenger RNAs[1,2] by moving processively along cytoskeletal actin filaments[3–5]. Because of the cell's dense and heterogeneous actin meshwork[6], the cargo itself should apply a dynamic load onto the myosin V. To overcome this load, a single myosin V converts the chemical free energy of 1 ATP into a directional motion of 36 nm and a maximum force of 2–3 pN[4,7,8]. Its structure is composed of a motor domain (or head domain), which includes the actin and nucleotide-binding site, a lever arm, which has six calmodulin-binding sites, and a tail domain, which is responsible for dimerization[9,10]. Finally, myosin V operates as a dimer.

The structural dynamics during unidirectional motion are well-characterized at the single molecule level[11–15]. Coupled with hydrolysis of ATP by the head, the two head domains alternately step 72 nm (hand-over-hand mechanism)[12] by combining the lever-arm swing by the lead (bound) head with a "diffusional Brownian search" by the rear (unbound) head[13,14,16] (Fig. 1). The lever-arm swing is a conformational change that drives forward motion and is accompanied by force. Although the diffusional Brownian search is a random and passive motion, a strong catch (strong binding) of the Brownian head to the forward actin target should also be accompanied by force. Because both mechanical processes are potentially force generating, it is necessary to quantify the work distribution between them to clarify the overall force generation mechanism used by myosin V. Here, to examine which of the lever-arm swing or Brownian search-and-catch is the greater force generator, we measured their respective energetic contributions.

Single molecule force measurement using DNA handle

Optical tweezers are a preferred method to quantify the force (or work) by a motor protein[17]. However, standard methods of this technique are not well suited for discriminating the work done by lever-arm swing and Brownian search-and-catch independently, because the optically-trapped bead used to monitor the motion is attached to the tail domain of myosin, far from the myosin head. To remedy this problem, we applied a DNA handle in our optical tweezers assay sys-

Corresponding author: Mitsuhiro Iwaki, Quantitative Biology Center, RIKEN, Suita, Osaka 565-0874, Japan.
e-mail: iwaki@fbs.osaka-u.ac.jp

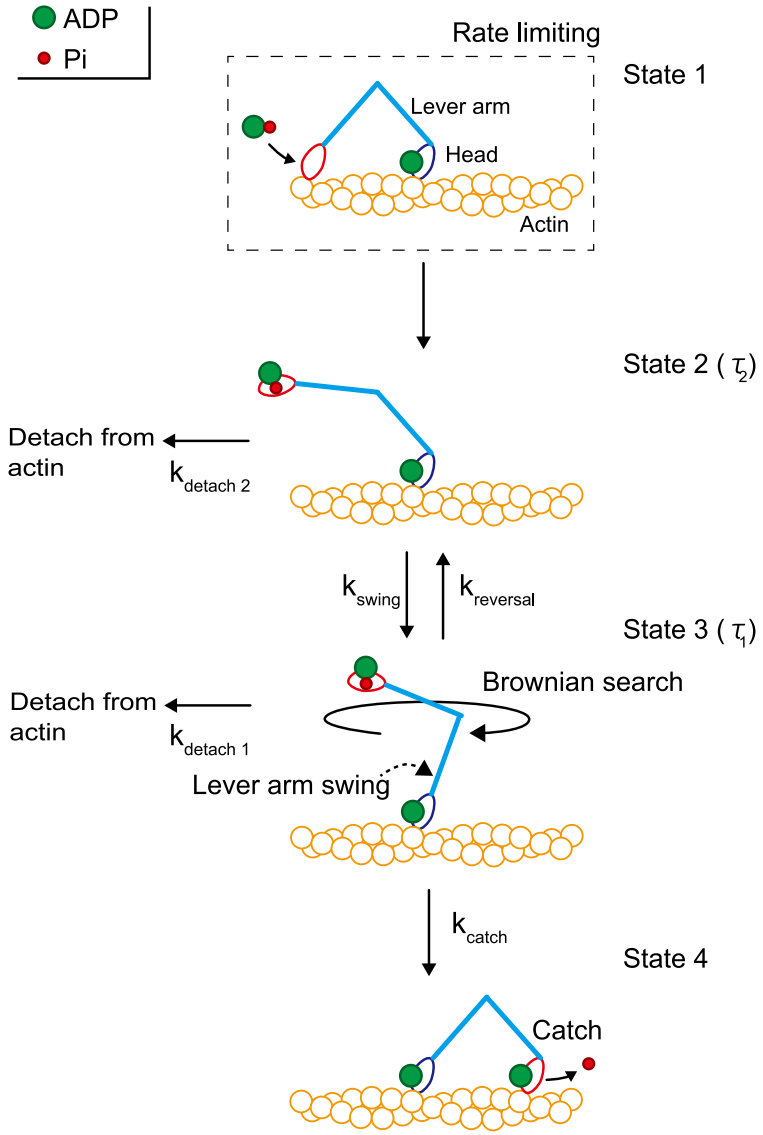

Figure 1 Hand-over-hand motion of myosin V. The rear head binds ATP and detaches from actin (state 1 → state 2 transition). A 20 nm sub-step of the rear (unbound) head results from a lever-arm swing (state 2 → state 3 transition). The detached head then undergoes a Brownian search-and-catch to bind to the next actin-binding site (state 3 → state 4 transition). ADP release from the rear head followed by attachment of new ATP molecule there returns us to state 1. At high load, the lever arm can also reverse its motion (state 3 → state 2 transition).

tem[18]. The DNA handle is composed of double-stranded DNA ~60 nm in length and tethers the myosin head directly to a 200-nm fluorescent polystyrene bead (Fig. 2a). The bead position is detected with nanometric and millisecond spatio-temporal resolution. Myosin V was observed walking along actin filaments using this setup[19].

In the presence of ATP, the observed 77 nm processive steps were decomposed into 20 and 57 nm sub-steps (Fig. 2b, inset). Because the duration of the sub-steps was 123 ms, which is comparable to the first-passage time of a Brownian head to reach the forward actin binding site 77 nm away under load and because the expected bead displacement from the lever-arm swing is 20 nm[20], we concluded the sub-steps to represent a 20 nm lever-arm swing and 57 nm Brownian search-and-catch.

Fluctuation in lever-arm swing under load

We also observed -20 nm sub-steps that coupled with the 20 nm lever-arm swing (Fig. 2c), suggesting these sub-steps are the result of a lever-arm reversal (Fig. 1, state 3 → state 2). The duration of state 3 and 2 in Figure 1, τ_1 and τ_2, respectively, were load-dependent and fit to a single exponential curve. The inverse of the duration describes the transition rates

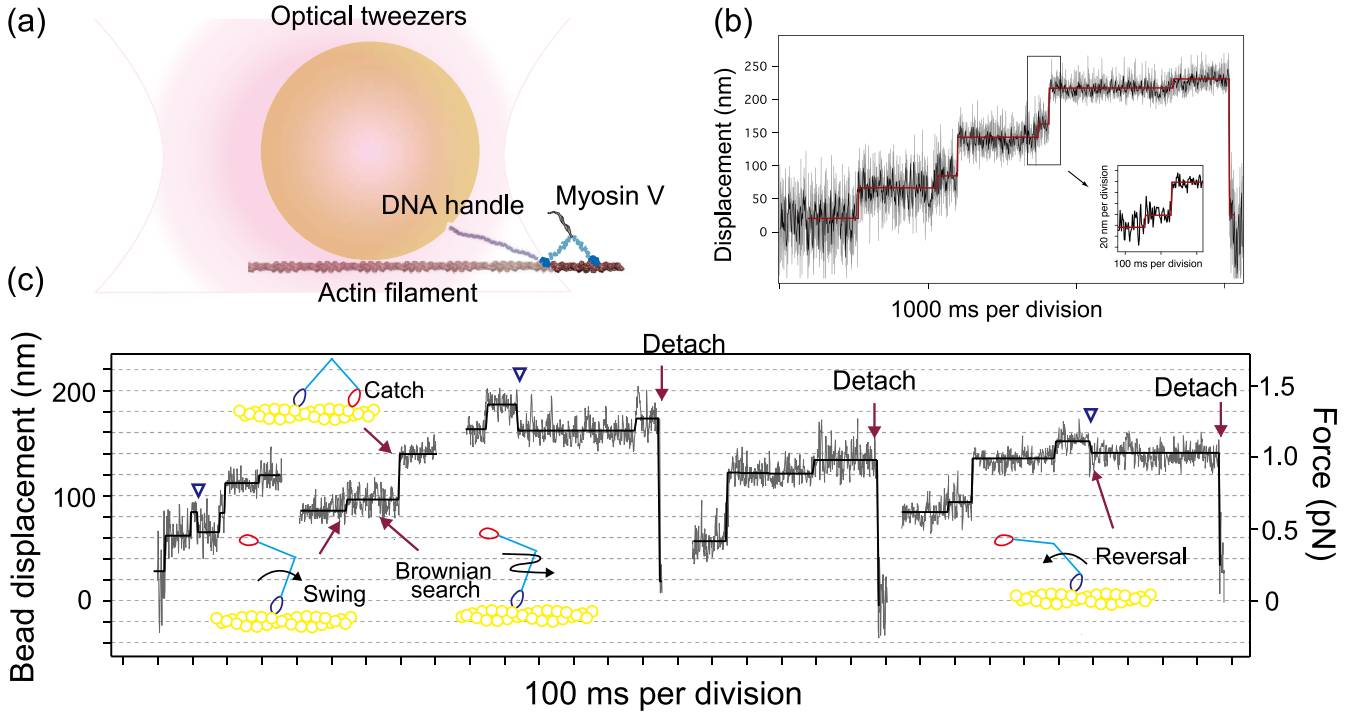

Figure 2 Optical tweezers assay using DNA handle. (a) Experimental setup. One end of a double-stranded DNA was biotinylated and attached to the amino terminus of a myosin V head via neutravidin. The opposite end was labelled with digoxigenin (DIG) and attached to a 200-nm fluorescent polystyrene bead coated with DIG antibodies. (b) Processive steps by single myosin V molecules at low ATP concentration (3 μM). Consecutive 20+57 nm sub-steps movements are seen. Grey trace, data low-pass filtered at 400 Hz. Individual steps (red line) were detected by a running t-test. Black trace, date median-filtered. Inset: sub-steps low-pass filtered at 200 Hz and enlarged. (c) Typical trajectories showing lever-arm swing and reversal at saturating ATP concentration (1 mM). Grey traces, data low-pass filtered at 400 Hz. Individual steps (black line) were detected by a running t-test. Arrow heads indicate –20 nm lever arm reversals.

$$\frac{1}{\tau_1} = k_{total1} = k_{reversal} + k_{catch} + k_{detach1}$$

$$\frac{1}{\tau_2} = k_{total2} = k_{swing} + k_{detach2}$$

The ratio of the rates correspond to the frequency of the observed events ($k_{reversal} : k_{catch} : k_{detach1} = N_{reversal} : N_{catch} : N_{detach1}$ and $k_{swing} : k_{detach2} = N_{swing} : N_{detach2}$), where N_i is the number of observations for state i. Figure 3a shows the normalized frequencies of the subsequent transition state used to estimate the transition rates.

Figure 3b shows the load dependent transition rates for the lever-arm swing and lever-arm reversal. The lever-arm swing involves a structural change that is opposed by the load. Therefore, the reaction rate decreases with increasing load in a manner that obeys an Arrhenius-type transition,

$$k(F) = k_0 e^{\left(\frac{-Fd}{k_B T}\right)}$$

where k_0 is the transition rate in the absence of load, F is force, d is the characteristic distance (force sensitivity), and k_BT is the thermal energy.

For similar reasons, load should promote lever-arm reversal, which is consistent with our observation that the transition rate slightly increases with increasing load. The fitting parameter, d, which relates to the force dependency of the reaction, indicates the lever-arm reversal is less sensitive to load than the lever-arm swing. Therefore, once the lever-arm has swung forward, it robustly maintains the post-lever-arm swing conformation when sensing load.

Lever-arm swing vs. Brownian search-and-catch

Given the individual rate constants, we can estimate the free-energy difference (ΔG) between the pre- and post-lever-arm swing states of the lead (bound) head using the formula

$$\frac{k_{reversal}}{k_{swing}} = e^{\left(\frac{\Delta G^0 - Fd}{k_B T}\right)}$$

where ΔG^0, F, d, k_B and T denote the free energy difference in the absence of load, force exerted by the optical tweezers, the characteristic distance, Boltzmann's constant and absolute temperature, respectively. At no load, which describes the maximum energy bias of the lever-arm swing, ΔG^0 was estimated to be –3.3 k_BT (Fig. 3c).

The work done by a myosin dimer can be divided into two parts, work done by structural changes in the lever-arm and work done by the Brownian search-and-catch. We showed hand-over-hand stepping is triggered by a 3.3 k_BT lever-arm

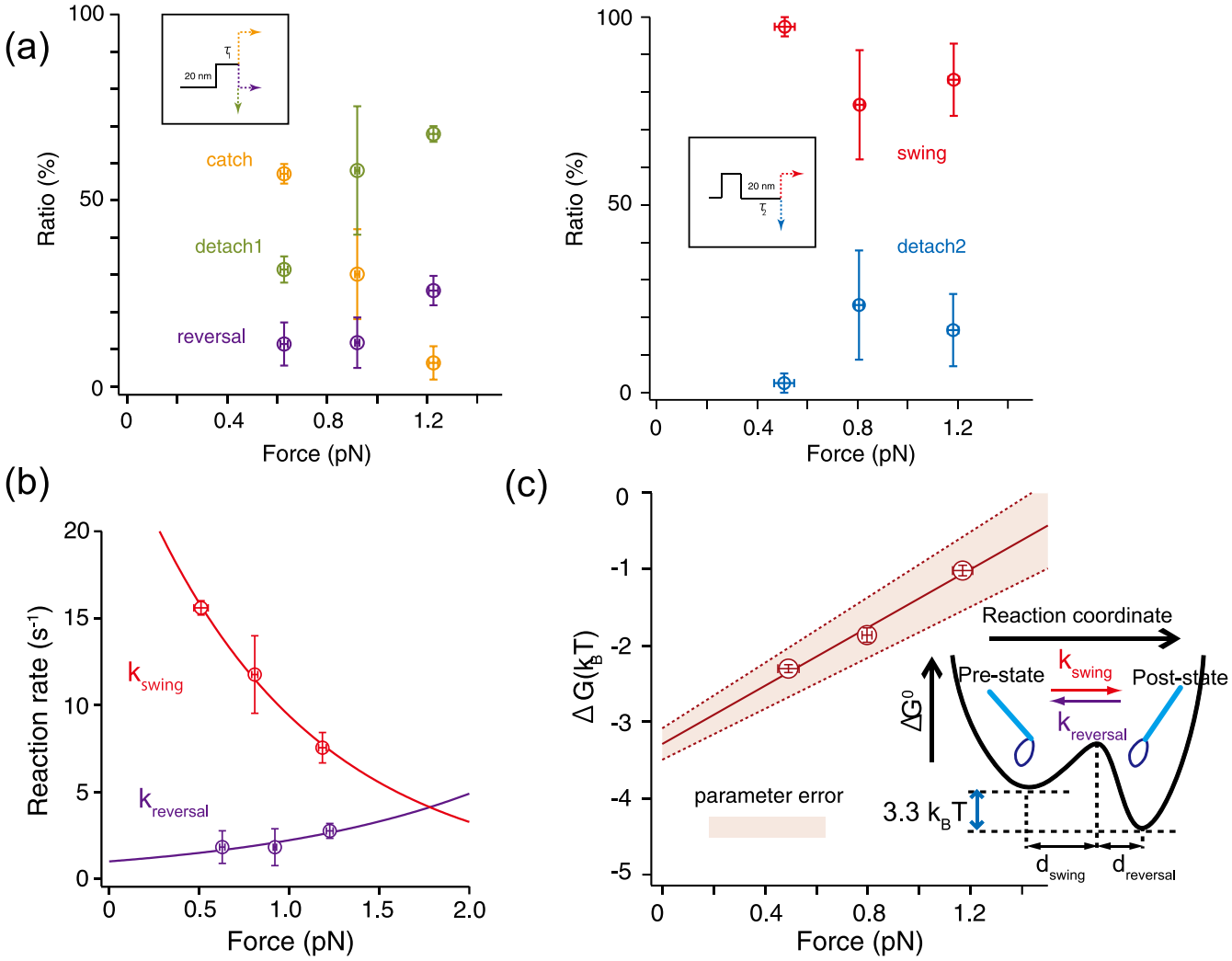

Figure 3 Structural stability of lever arm for myosin V. (a) The normalized frequency of each transition state from the post- (left) and pre- (right) lever-arm swing states. The frequency of each transition was experimentally obtained by counting the number of reactions. Error bars show the standard error of the mean (SEM). (b) Load dependent reaction rates for the lever-arm swing (k_{swing}) and the reversal ($k_{reversal}$). The load dependency can be described as a single exponential. The characteristic distances, $d_{reversal}$ and d_{swing}, are –2.9 nm and 5.9 nm, respectively, meaning the energy barrier between the two states is asymmetrical. Thus, the lever arm reversal is more robust to load than the lever-arm swing. (c) The load dependent free energy difference (ΔG) between the pre- and post-lever-arm swing states. Error bars show SEM. Inset: free energy landscape of the two-state lever arm model.

swing in the lead (bound) head. The Brownian search-and-forward-catch contributes work to this system as load is exerted onto the myosin molecule. During physiological vesicle transport, myosin V apparently distributes the load from a cargo bound to the tail domain completely onto the lead (bound) head. However, when the rear (unbound) head undergoes Brownian motion, the lever-arm in the lead (bound) head should bend 10–15 nm backwards when a 2–3 pN load is exerted (bending stiffness = ~0.2 pN/nm)[21]. In these cases, the Brownian head will conduct work when it catches an actin target 77 nm forward. Therefore, the work done by the Brownian search-and-catch is physiologically relevant. We found that the majority of myosin V molecules completed the Brownian search-and-catch against 0.93 pN on average (data not shown). This equates to a Brownian search-and-catch contribution of 13 k_BT (57 nm × 0.9 pN) of work, which is similar to the chemical free energy from Pi release (12 k_BT)[22] when a myosin head strongly catches forward actin. Consequently, myosin V predominantly works during the Brownian component by controlling Pi release, while the structural change of the lever-arm is a trigger for the forward catch. Supporting this theory, we reproduced 2–3 pN stall force and 18 k_BT total work at the tail loading condition in a Langevin dynamics simulation using a 3.3 k_BT energy bias in the lever-arm swing and experimentally obtained the transition rate constants[19].

Strain sensor as a rectifier of Brownian motion

How does Brownian head ensure a strong catch? We have previously proposed the "strain sensor mechanism"[23], which explains the decision-making by the Brownian head. We describe it briefly below.

It is known that when the Brownian head is bound to both ADP and Pi, it undergoes weak interactions with actin, which can be described as an equilibrium state between rapid (sub millisecond) attachments and detachments[24]. We constructed an ultrafast optical tweezers assay[23] that can directly observe the weak binding state by detecting weak attachments between myosin and actin. We applied this system to myosin VI, which moves the opposite direction of myosin V, and found that Pi release, which corresponds with the transition from weak to strong binding, was very mechano-sensitive. When backward load (opposite direction to the myosin movement) was applied to a weak-binding head, the strong binding was greatly accelerated (~30-fold), whereas forward load did not affect the weak-to-strong transition rate. In the case of dimeric myosin V and VI, intramolecular strain should occur when forming a two-headed bound state (Fig. 1, states 1 and 4). When the Brownian head spans the actin helical pitch and forms a two-headed bound state, the rear head senses a forward strain and the weakly-attached front head senses a backward strain. Because the backward load accelerates strong binding, the forward catch is ensured.

We have proposed a model to explain how strong binding is accelerated in a strain-dependent manner[23]. The opening and closing of the exit route for Pi, termed the "back door"[25], has been mechanically linked to that of the nucleotide (ATP or ADP)-binding pocket, or "front door"[26]. The strain dependencies of the ADP release and ATP binding rates have previously been measured[27–29], revealing that external force applied to the head strains the front door. When the lever-arm is pulled backward, the head is bent forward, which closes the front door and opens the back door. Thus, backward strain accelerates Pi release and hence strong binding. At the same time, closing of the front door suppresses ADP release or ATP binding[29], which means the overall ATP turnover rate is slow under backward load. On the other hand, upon forward strain, the backdoor is closed or unaffected, resulting in a relatively rare transition to strong binding. This strain-dependent, asymmetric catch mechanism should be important for the Brownian head's reliable forward movement.

We believe the structure-based mechanism of the strain sensor should be applicable to not only myosin VI but myosin V. It is known that the lever arm of myosin VI is bent 180 degrees, which distinguishes it from myosin V, and that this bend is responsible for the different direction of movement[30]. Because the angle between the lever-arm and head should be important for the opening and closing of the front and back doors, we propose the relationship between the opening and closing between the two myosins are opposite based on the different positions of the lever arms.

To explicitly examine the relationship between the direction of myosin movement and the strain-sensor mechanism, we applied our ultrafast optical tweezers assay to myosin V. The results of the myosin V experiments are in agreement with our model, which assumes backward strain accelerates strong binding (unpublished data). Therefore, the strain-sensor mechanism should contribute to the directionality of the myosin motor.

The strain sensor mechanism is notable in that random Brownian motion is rectified in one direction by sensing the intensity and direction of the mechanical strain. Using this simple mechanism, myosin can autonomously sense positional information and adaptably respond to changes in its environment. These characteristics should be important in motor assembly systems like muscle.

Physiological advantages of the Brownian machine

Figure 4 shows the contribution of the lever-arm swing and Brownian search-and-forward catch to myosin V work at various loads when assuming physiological vesicle transport geometry (vesicle is attached at the tail domain). When 0.5 pN force is applied to the tail end, the lever-arm swing conducts 2.4 k_BT (20 nm × 0.5 pN) of work, whereas the total work done by myosin V is 4.4 k_BT (36 nm × 0.5 pN), meaning the Brownian search-and-catch component contributes 2.0 k_BT. Although the amount of work done by the lever-arm swing increases with load, it never exceeds 3.3 k_BT at saturating physiological ATP concentration. Any residual work at high loads then is done by the Brownian search-and-catch. Thus, our results argue the myosin V is a lever-arm-driven motor under low loads, but a Brownian search-and-catch driven motor under high loads. This result suggests that myosin V can change its force-generating mechanism depending on the external force.

Knowing that the vast majority of work done by myosin V at high load is a stochastic process (Brownian search-and-catch) and that the proportion of work done by the deterministic lever-arm swing and Brownian search-and-catch varies with load offers important insights into the mechanisms used by myosin V for its function. The hand-over-hand steps caused by deterministic lever-arm swings would be advantageous for smooth, rapid movement at near-zero load when no obstacles are present. However, cells contain a cytoskeleton meshwork and a number of dynamic molecules and vesicles that risk disturbing transport[31]. In these cases, the Brownian search-and-catch mechanism should be advantageous for avoiding such obstructions. Thus, our findings indicate that myosin V is an optimized nanomachine highly adaptable to its intracellular environment, which should have significant implications on the design of artificial nanomotors.

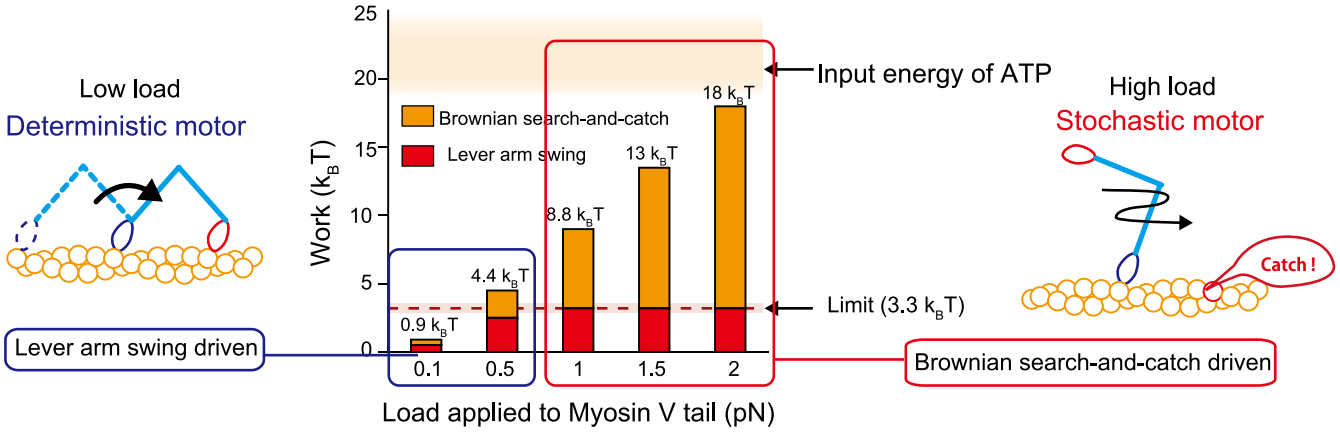

Figure 4 Work distribution of myosin V at different loads applied to the tail. Whereas the work done by the Brownian search-and-catch increases with load, that done by the lever arm is constrained by the energy difference between the pre- and post-lever-arm swing states.

Perspectives

To conclude, we have succeeded to quantify both the bias energy of the lever-arm swing and the work done by the Brownian search-and-catch. Surprisingly, the bias energy of the lever-arm swing (~3 k_BT) was much smaller than expected according to the lever-arm swinging model (>10 k_BT)[32,33]. Instead, inherent Brownian motion is the dominant driving force. This motion is rectified by steric compatibility between the myosin head and actin filament[34] or by a strain sensor mechanism coupled with Pi release. The requisite energy to work is temporarily supplied from a thermal bath (Brownian motion) and forward diffusion is locked by consuming the chemical free energy of Pi release. In this sense, myosin V is a Brownian machine that can adjust its function in response to environmental change. This design should be advantageous for constructing artificial systems in which individual components autonomously coordinate to achieve efficient and adaptable function.

Accordingly, we are constructing an artificial muscle system using DNA nanotechnology called DNA origami[35]. DNA origami is an attractive tool in that it can be used to create three-dimensional nanostructures[36]. Regarding an artificial muscle system, we can attach myosin heads to DNA origami, which acts as an artificial thick filament (assembly of muscle myosin). Using DNA origami allows us to control not only the number of myosin heads, but also the spacing between heads. This model will be applied to studying the design principles of the muscle architecture, including how multiple Brownian machines achieve autonomous biological function in concert.

Acknowledgements

We thank colleagues of the Riken Quantitative Biology Center for discussions and Peter Karagianins for reading the manuscript. This work was supported by Grant-in-Aid for Scientific Research on Innovative Areas (to M.I.), Grant-in-Aids for Young Scientists (B) (to M.I.).

References

1. Reck-Peterson, S. L., Provance, D. W., Jr., Mooseker, M. S. & Mercer, J. A. Class V myosins. *Biochim. Biophys. Acta* **1496**, 36–51 (2000).
2. Vale, R. D. The molecular motor toolbox for intracellular transport. *Cell* **112**, 467–480 (2003).
3. Mehta, A. D., Rock, R. S., Rief, M., Spudich, J. A., Mooseker, M. S. & Cheney, R. E. Myosin-V is a processive actin-based motor. *Nature* **400**, 590–593 (1999).
4. Rief, M., Rock, R. S., Mehta, A. D., Mooseker, M. S., Cheney, R. E. & Spudich, J. A. Myosin-V stepping kinetics: a molecular model for processivity. *Proc. Natl. Acad. Sci. USA* **97**, 9482–9486 (2000).
5. Sakamoto, T., Amitani, I., Yokota, E. & Ando, T. Direct observation of processive movement by individual myosin V molecules. *Biochem. Biophys. Res. Commun.* **272**, 586–590 (2000).
6. Svitkina, T. M., Verkhovsky, A. B., McQuade, K. M. & Borisy, G. G. Analysis of the actin-myosin II system in fish epidermal keratocytes: mechanism of cell body translocation. *J. Cell Biol.* **139**, 397–415 (1997).
7. Kad, N. M., Trybus, K. M. & Warshaw, D. M. Load and Pi control flux through the branched kinetic cycle of myosin V. *J. Biol. Chem.* **283**, 17477–17484 (2008).
8. Uemura, S., Higuchi, H., Olivares, A. O., De La Cruz, E. M. & Ishiwata, S. Mechanochemical coupling of two substeps in a single myosin V motor. *Nat. Struct. Mol. Biol.* **11**, 877–883 (2004).
9. Cheney, R. E., O'Shea, M. K., Heuser, J. E., Coelho, M. V., Wolenski, J. S., Espreafico, E. M., Forscher, P., Larson, R. E. & Mooseker, M. S. Brain myosin-V is a two-headed unconventional myosin with motor activity. *Cell* **75**, 13–23 (1993).
10. Liu, J., Taylor, D. W., Krementsova, E. B., Trybus, K. M. & Taylor, K. A. Three-dimensional structure of the myosin V inhibited state by cryoelectron tomography. *Nature* **442**, 208–211 (2006).
11. Forkey, J. N., Quinlan, M. E., Shaw, M. A., Corrie, J. E. & Goldman, Y. E. Three-dimensional structural dynamics of myosin V by single-molecule fluorescence polarization. *Nature* **422**, 399–404 (2003).

12. Yildiz, A., Forkey, J. N., McKinney, S. A., Ha, T., Goldman, Y. E. & Selvin, P. R. Myosin V walks hand-over-hand: single fluorophore imaging with 1.5-nm localization. *Science* **300**, 2061–2065 (2003).
13. Shiroguchi, K. & Kinosita, K., Jr. Myosin V walks by lever action and Brownian motion. *Science* **316**, 1208–1212 (2007).
14. Dunn, A. R. & Spudich, J. A. Dynamics of the unbound head during myosin V processive translocation. *Nat. Struct. Mol. Biol.* **14**, 246–248 (2007).
15. Kodera, N., Yamamoto, D., Ishikawa, R. & Ando, T. Video imaging of walking myosin V by high-speed atomic force microscopy. *Nature* **468**, 72–76 (2010).
16. Nishikawa, S., Arimoto, I., Ikezaki, K., Sugawa, M., Ueno, H., Komori, T., Iwane, A. H. & Yanagida, T. Switch between large hand-over-hand and small inchworm-like steps in myosin VI. *Cell* **142**, 879–888 (2010).
17. Svoboda, K. & Block, S. M. Force and velocity measured for single kinesin molecules. *Cell* **77**, 773–784 (1994).
18. Guydosh, N. R. & Block, S. M. Direct observation of the binding state of the kinesin head to the microtubule. *Nature* **461**, 125–128 (2009).
19. Fujita, K., Iwaki, M., Iwane, A. H., Marcucci, L. & Yanagida, T. Switching of myosin-V motion between the lever-arm swing and brownian search-and-catch. *Nat. Commun.* **3**, 956 (2012).
20. Coureux, P. D., Wells, A. L., Menetrey, J., Yengo, C. M., Morris, C. A., Sweeney, H. L. & Houdusse, A. A structural state of the myosin V motor without bound nucleotide. *Nature* **425**, 419–423 (2003).
21. Veigel, C., Schmitz, S., Wang, F. & Sellers, J. R. Load-dependent kinetics of myosin-V can explain its high processivity. *Nat. Cell Biol.* **7**, 861–869 (2005).
22. Howard, J. *Mechanics of Motor Proteins and the Cytoskeleton*. (Sinauer Associates, Sunderland, 2001).
23. Iwaki, M., Iwane, A. H., Shimokawa, T., Cooke, R. & Yanagida, T. Brownian search-and-catch mechanism for myosin-VI steps. *Nat. Chem. Biol.* **5**, 403–405 (2009).
24. Brenner, B. Rapid dissociation and reassociation of actomyosin cross-bridges during force generation: a newly observed facet of cross-bridge action in muscle. *Proc. Natl. Acad. Sci. USA* **88**, 10490–10494 (1991).
25. Yount, R. G., Lawson, D. & Rayment, I. Is myosin a "back door" enzyme? *Biophys. J.* **68**, 44S–47S; discussion 47S–49S (1995).
26. Holmes, K. C., Angert, I., Kull, F. J., Jahn, W. & Schroder, R. R. Electron cryo-microscopy shows how strong binding of myosin to actin releases nucleotide. *Nature* **425**, 423–427 (2003).
27. Veigel, C., Molloy, J. E., Schmitz, S. & Kendrick-Jones, J. Load-dependent kinetics of force production by smooth muscle myosin measured with optical tweezers. *Nat. Cell Biol.* **5**, 980–986 (2003).
28. Oguchi, Y., Mikhailenko, S. V., Ohki, T., Olivares, A. O., De La Cruz, E. M. & Ishiwata, S. Load-dependent ADP binding to myosins V and VI: implications for subunit coordination and function. *Proc. Natl. Acad. Sci. USA* **105**, 7714–7719 (2008).
29. Altman, D., Sweeney, H. L. & Spudich, J. A. The mechanism of myosin VI translocation and its load-induced anchoring. *Cell* **116**, 737–749 (2004).
30. Bryant, Z., Altman, D. & Spudich, J. A. The power stroke of myosin VI and the basis of reverse directionality. *Proc. Natl. Acad. Sci. USA* **104**, 772–777 (2007).
31. McGuffee, S. R. & Elcock, A. H. Diffusion, crowding & protein stability in a dynamic molecular model of the bacterial cytoplasm. *PLoS Comput. Biol.* **6**, e1000694 (2010).
32. Spudich, J. A. How molecular motors work. *Nature* **372**, 515–518 (1994).
33. Spudich, J. A. The myosin swinging cross-bridge model. *Nat. Rev. Mol. Cell Biol.* **2**, 387–392 (2001).
34. Kinosita, K., Ali, M. Y., Adachi, K., Shiroguchi, K. & Itoh, H. How two-foot molecular motors may walk. *Adv. Exp. Med. Biol.* **565**, 205–219 (2005).
35. Rothemund, P. W. Folding DNA to create nanoscale shapes and patterns. *Nature* **440**, 297–302 (2006).
36. Douglas, S. M., Dietz, H., Liedl, T., Hogberg, B., Graf, F. & Shih, W. M. Self-assembly of DNA into nanoscale three-dimensional shapes. *Nature* **459**, 414–418 (2009).